HHS Public Access

Author manuscript

Neurobiol Dis. Author manuscript; available in PMC 2022 January 01.

Published in final edited form as:

Neurobiol Dis. 2021 January ; 148: 105216. doi:10.1016/j.nbd.2020.105216.

MANF is Neuroprotective against Ethanol-induced Neurodegeneration through Ameliorating ER Stress

Yongchao Wang[1], **Wen Wen**[2], **Hui Li**[2], **Marco Clementino**[3], **Hong Xu**[4], **Mei Xu**[4], **Murong Ma**[4], **Jacqueline Frank**[5], **Jia Luo**[2,6,#]

[1]Department of Cell and Development Biology, Vanderbilt University School of Medicine, Nashville, TN 37232

[2]Department of Pathology, University of Iowa Carver College of Medicine, Iowa City, IA 52242

[3]Department of Toxicology and Cancer Biology, University of Kentucky College of Medicine, Lexington, KY 40536

[4]Department of Pharmacology and Nutritional Sciences, University of Kentucky College of Medicine, Lexington, KY 40536

[5]Department of Neurology, University of Kentucky College of Medicine, Lexington, KY 40536

[6]Iowa City VA Health Care System, Iowa City, IA 52246

Abstract

Fetal alcohol spectrum disorders (FASD) are a spectrum of developmental disorders caused by prenatal alcohol exposure. Neuronal loss or neurodegeneration in the central nervous system (CNS) is one of the most devastating features in FASD. It is imperative to delineate the underlying mechanisms to facilitate the treatment of FASD. Endoplasmic reticulum (ER) stress is a hallmark and an underlying mechanism of many neurodegenerative diseases, including ethanol-induced neurodegeneration. Mesencephalic astrocyte-derived neurotrophic factor (MANF) responds to ER stress and has been identified as a protein upregulated in response to ethanol exposure during the brain development. To investigate the role of MANF in ethanol-induced neurodegeneration and its association with ER stress regulation, we established a CNS-specific *Manf* knockout mouse model and examined the effects of MANF deficiency on ethanol-induced neuronal apoptosis and ER stress using a third-trimester equivalent mouse model. We found MANF deficiency exacerbated

[#]Corresponding author: Jia Luo, Department of Pathology, University of Iowa Carver College of Medicine, Iowa City, IA 52242; jia-luo@uiowa.edu; Tel: 319-335-2256;.

Yongchao Wang: Conceptualization, Methodology, Data curation, Writing-Original draft preparation, Writing-Reviewing and Editing
Wen Wen: Methodology, Investigation, Writing-Reviewing and Editing
Hui Li: Methodology, Investigation
Marco Clementino: Data curation
Hong Xu: Methodology, Investigation
Mei Xu: Methodology, Investigation
Murong Ma: Methodology, Investigation
Jacqueline Frank: Methodology, Investigation
Jia Luo: Conceptualization, Writing-Reviewing and Editing, Funding acquisition, Project administration

ethanol-induced neuronal apoptosis and ER stress and that blocking ER stress abrogated the harmful effects of MANF deficiency on ethanol-induced neuronal apoptosis. Moreover, using an animal model of ER-stress-induced neurodegeneration, we demonstrated that MANF deficiency potentiated tunicamycin (TM)-induced ER stress and neurodegeneration. A whole transcriptome RNA sequencing also supported the functionality of MANF in ER stress modulation and revealed targets that may mediate the ER stress-buffering capacity of MANF. Collectively, these results suggest that MANF is a neurotrophic factor that can protect neurons against ethanol-induced neurodegeneration by ameliorating ER stress.

Keywords

Alcohol abuse; apoptosis; brain; development; unfolded protein response

Introduction

Fetal alcohol spectrum disorders (FASD) represent a spectrum of disorders resulted from prenatal alcohol exposure (Lebel *et al.* 2011; Mattson *et al.* 2013). In the United States, around 2–5% of babies are born with FASD each year (May *et al.* 2018). The CNS development is a complex and exquisitely orchestrated process. Developmental exposure to alcohol impacts this process, which is manifested by learning and memory deficits as well as other neuropathology (Kane & Drew 2020; Mattson *et al.* 2011). Imaging studies reveal alterations of structure and neural circuitry in brain regions like the hippocampus, cerebral cortex, and cerebellum (Joseph *et al.* 2014; Norman *et al.* 2009). The structural changes in the hippocampus and cerebrum are correlated with the severity of cognitive dysfunction, whereas damages to the cerebellum are associated with motor dysfunction and cerebellar-linked cognitive deficits (Connor *et al.* 2006; Diwadkar *et al.* 2013; Glass *et al.* 2014). The effects of structural damage on the CNS are long-lasting; individuals with FASD are more likely to develop substance abuse and mood disturbances in adulthood (Mattson *et al.* 2011). Fetal exposure of ethanol can predispose CNS to increased neurodegeneration and altered synaptic plasticity that are concomitant with cognitive and behavioral deficits (Patten *et al.* 2014; Ke *et al.* 2011).

Multiple mechanisms have been proposed for ethanol-induced neurodegeneration; oxidative stress and neuroinflammation are regarded as the important ones (Lucas *et al.* 2006; Qin *et al.* 2008; Qin & Crews 2012; Crews & Nixon 2009). Ethanol can cross the blood-brain barrier (BBB) and consequently activates nuclear factor kappa-light-chain-enhancer of activated B cells (NF-κβ)-mediated inflammatory response (Crews & Vetreno 2016). Inflammatory cytokines or substances such as high mobility group box 1 (HMGB1) and damage-associated molecular patterns (DAMPs) are released from microglial cells to activate toll-like receptors (TLRs) and receptor for advanced glycation end products (RAGE) that, in turn, further promote NF-κβ mediated inflammatory response (Crews & Vetreno 2016). Moreover, ethanol can induce inflammation in the liver and cause a systemic inflammation; the induced inflammatory cytokines, e.g., tumor necrosis factor-alpha (TNFα), can cross BBB through receptor-mediated transportation and contribute to the existing inflammation in the brain (Crews & Vetreno 2016; Ferrier *et al.* 2006). Ethanol

exposure can also produce oxidative stress, which is devastating. Oxidative stress may cause neuronal death directly or interact with the inflammatory pathway to potentiate the harmful effects of neuroinflammation (Morgan & Liu 2011; Kratsovnik *et al.* 2005). It has also been reported that oxidative stress can inhibit neurogenesis and thereby indirectly contributes to neuronal loss (Crews & Vetreno 2016).

Endoplasmic reticulum (ER) regulates protein folding; only properly folded proteins can pass through quality control surveillance and shuttle to the Golgi compartment. Misfolded proteins are retained in ER through interactions with chaperones and eventually targeted for degradation either by the ubiquitin-proteasome system (UPS) or by the autophagy-lysosome system. The overload of unfolded or misfolded protein in ER resulted from various conditions, such as pathogen infection, nutrient deprivation, inflammation, alterations in ER luminal Ca^{2+} or redox status, and toxic chemicals can cause ER stress (Ron 2002). ER stress activates an unfolded protein response (UPR) to eliminate unfolded or misfolded proteins in the ER. The UPR is regulated through three ER-localized transmembrane proteins, Inositol-requiring kinase (IRE1), protein kinase RNA-like endoplasmic reticulum kinase (PERK), and activating transcription factor 6 (ATF6) (Marciniak & Ron 2006). When ER stress is excessively activated, and the cellular function cannot be restored, it leads to cell death (Hetz & Saxena 2017). Accumulation of misfolded protein is a sharing characteristic of many neurodegenerative diseases such as Parkinson's disease, Alzheimer's disease, Huntington's disease, and Amyotrophic Lateral Sclerosis (ALS) (Hetz & Saxena 2017; Aguzzi & O'Connor 2010). ER stress has been implicated as one of the underlying mechanisms for these neurodegenerative diseases. With a variety of preclinical models, targeting UPR through pharmacological and genetic approaches in these diseases generated profound effects on the outcomes of these diseases (Hetz & Saxena 2017). Ethanol-induced ER stress is linked with multiple organ injuries; ER stress is found in acute pancreatitis (Kubisch *et al.* 2006; Pandol *et al.* 2010; Lugea *et al.* 2011), ethanol-induced liver disease (ALD) (Ji & Kaplowitz 2006; Ji *et al.* 2011; Dara *et al.* 2011; Ji *et al.* 2005), and the myocardium of ethanol-fed mice (Li & Ren 2008). ER stress is induced by ethanol exposure in both adult and developing mouse brain. Moreover, blockage of ER stress with pharmacological inhibitors reduces ethanol-induced neurodegeneration, indicating that ER stress contributes to ethanol-induced neurodegeneration (Ke *et al.* 2011; Wang *et al.* 2018).

MANF, also recognized as arginine-rich mutated in early stages of tumor (ARMET), was identified in a ventral mesencephalic astrocyte cell line 1 in search of astrocyte-derived neurotrophic factor (Petrova *et al.* 2003). MANF is widely expressed in the cerebral cortex, hippocampus, and cerebellum and can also be detected in the liver, kidney, and testes (Lindholm *et al.* 2008). The crystal structure of mammalian MANF has revealed that MANF contains several motifs: a saposin-like domain in the amino-terminal, an SAP-like domain in the carboxy-terminal and a C-X-X-C motif. The saposin-like domain can interact with lipid and membrane, thereby linking MANF to the ER membrane. The SAP-like domain shares high homology with the SAP domain in Ku70 and has been reported to interact with proapoptotic proteins such as Bad and Bax to inhibit their function. The C-X-X-C motif is commonly found in protein disulfide isomerase, mediating the formation of disulfide bonds (Hellman *et al.* 2011; Hoseki *et al.* 2010). MANF is involved in neural development, such as neurite outgrowth and neuronal migration (Tseng *et al.* 2017). MANF has been found to

have trophic effects on embryonic dopaminergic neurons both *in vitro* and *in vivo* (Petrova *et al*. 2003; Voutilainen *et al*. 2009; Lindholm & Saarma 2010). Neves *et al*. shows that MANF is induced in innate immune cells during retina injury; the induced MANF is involved in the alternative activation of microglial cells, which is essential for retinal repair and regeneration (Neves *et al*. 2016). It has also been shown that MANF can cause insulin resistance in the neurons of the hypothalamus, thereby increasing food intake and causing hyperphagia phenotype in mice (Yang *et al*. 2017). Meantime, MANF has been found to respond to ER stress and identified as a protein upregulated by UPR (Apostolou *et al*. 2008). It is upregulated in myocardial infarction and brain diseases such as cerebral epilepsy, and ischemia wherein ER stress is a sharing characteristic (Lindholm *et al*. 2008; Yu *et al*. 2010; Tadimalla *et al*. 2008).

We demonstrated that MANF was induced in the developing mouse brain after ethanol exposure (Li *et al*. 2019; Ke *et al*. 2011). We hypothesized that MANF was associated with ER stress regulation and protective against ethanol-induced neurodegeneration. In the present study, we investigated the role of MANF in ER stress and its association with ethanol-induced neuronal damage using a well-established third-trimester equivalent mouse model.

Materials and Methods

Reagents and antibodies

Reagents for blood ethanol levels were purchased from Analox Instruments (London, UK). ATF6 was purchased from Life Span Biosciences (Seattle, WA). Cleaved caspase-3 was from Cell Signaling Technology (Danvers, MA). GRP78 antibody was from Novus Biologicals (Littleton, CO). X-box binding protein-1s (XBP1s) antibody was from BioLegend (San Diego, CA). MANF antibody was from Abcam (Cambridge, MA). CCAAT/enhancer-binding protein homologous protein (CHOP) antibody was from Thermo Fisher Scientific (Rockford, IL). HRP-conjugated anti-rabbit and anti-mouse secondary antibodies were from GE Healthcare Life Sciences (Piscataway, NJ). Mounting media containing 4′, 6-diamidino-2-phenylindole (DAPI) was from Vector Laboratories (Burlingame, CA). Alexa-488 conjugated anti-rabbit and Alexa-594 conjugated anti-mouse antibodies were from Life Technologies (Grand Island, NY). Ketamine/xylazine was from Butler Schein Animal Health (Dublin, OH). Other chemicals and reagents were purchased either from Sigma-Aldrich or Life Technologies (Frederick, MD).

Animal model

Central nervous system specific *Manf* knockout—Embryonic stem cell clone EPD0162_3_D06 (*Manf*$^{tm1a(KOMP)Wtsi}$) as illustrated in Figure 1 was generated by the Wellcome Sanger Institute and injected into blastocyst by the Knockout Mouse Project (KOMP) Repository and the Mouse Biology Program at the University of California (UC) Davis. The generated chimeric mice were then bred with C57BL/6N mates. Then via UC Davis Mouse Biology Program, MANF mice were crossed with an FLP recombinase line for *in vivo* recombination to convert to the conditional (floxed) allele. The FLP recombinase line was obtained from the MMRRC: C57BL/6-Tg(CAG-Flpo)1Afst/Mmucd, 032247-UCD.

Two generations of breeding were performed to ensure excision in the germ cells and remove the FLP transgene. They also bred to homozygosity at our request. Nestin-Cre$^{+/-}$ transgenic mice (B6.Cg-Tg(Nes-Cre)1Kln/J) were obtained from Jackson Laboratory. *Manf* $^{flox/flox}$ mice were first crossed with Nestin-Cre$^{+/-}$ mice to generate *Manf* $^{flox/+}$::Nestin-Cre $^{+/-}$ mice. Then the offspring were crossed with *Manf* $^{flox/flox}$ mice to generate *Manf* $^{flox/flox}$::Nestin-Cre$^{+/-}$ mice in which *Manf* was specifically knocked out in the central nervous system. For genotyping, mice tail genomic DNA was extracted using Fast Tissue/ Tail PCR Genotyping Kit (EZ BioResearch) according to the manufacturer's instructions. Primers used for genotyping are as follows: *Manf-f2*, GAGATGGCGCAACGCAATTAATG; *Manfr2*, CCATGGTGATGCTGTAACTGTCACG; *Manf-r1*, TGCTCAGCTGCAGAGTTAGAGTTCC; *Manf-f1*, TGAAGCAAGAGGCAAAGAGAATCGG. *Cre*-F, GGTTCGCAAGAACCTGATGG; *Cre*-R, GCCTTCTCTACACCTGCGG. Touch-Down PCR protocol was used for the reactions. For the first 10 cycles which annealed at 65°C decreasing in temperature by 1°C per cycle and an additional 30 cycles annealed at 55 °C. The amplifications were performed in 12 μl volume, and the PCR cycles were 94°C for 5 min, 94°C for 15 sec, annealing for 30 sec, 72°C for 40 sec and final extension 72°C for 5 min. The length of amplified bands for *Manf* $^{+/+}$, *Manf* $^{flox/flox}$ (CTL), and conditional *Manf* $^{flox/flox}$::Cre$^{+/-}$ (cKO) targeted locus are listed as in Figure 1.

Ethanol- and TM-induced neurodegeneration in mice—All experimental procedures were approved by the Institutional Animal Care and Use Committee (IACUC) at the University of Kentucky (#2008–0401) and performed following regulations for the Care and Use of Laboratory Animals set forth by the National Institutes of Health (NIH) Guide. Two animal models were used in this study to investigate the effects of MANF on ER stress-induced neuronal damage: ethanol-induced neurodegeneration and TM-induced neurodegeneration. In ethanol-induced neurodegeneration, postnatal day (PD)7 pups (CTL and cKO) were randomly assigned to two groups: control and ethanol group; they were injected with PBS or ethanol (1.5 g/kg, 20% solution in PBS) subcutaneously twice at a two-hour interval. Neuronal apoptosis and ER stress were assessed 8 hours after the first injection. In TM-induced neurodegeneration, PD7 pups (CTL and cKO) were injected with 150 mM dextrose (Mock treatment) or TM (3 mg/kg, 30% solution in dextrose) subcutaneously once. Neuronal apoptosis and ER stress were assessed 24 hours after the injection. For inhibition of ER stress with sodium phenylbutyrate (4-PBA), PD6 pups (CTL and cKO) were injected with 4-PBA or PBS subcutaneously twice at a dose of 100 mg/kg 24 hours and 2 hours in advance and then subjected to ethanol or TM treatment following the same procedure as above. Neuronal apoptosis and ER stress in the brain from the CTL group and cKO mice were evaluated with immunoblotting and immunohistochemistry of ER stress markers and apoptotic markers as well as TUNEL assay. The experimenters were blinded to group assignment (control or experimental group).

Measurement of blood ethanol concentration (BEC)

One hour after ethanol injection, blood samples were collected from the tail vein. The blood was centrifuged, and 10 ul of the plasma was used to measure BEC using an Analox AM 1 analyzer (Lunenburg, MA) as previously described (Xu *et al.* 2016).

Immunoblotting

Brain tissues were collected, and proteins were extracted. Around 30–50 μg of extracted protein was used in immunoblots to examine the levels of ER stress markers (GRP78, CHOP, XBP1s, and ATF6), MANF, and apoptotic markers (cleaved caspase-3). The nitrocellulose membranes were first probed with specific primary antibodies overnight at 4°C. After washing with phosphate-buffered saline (PBS) containing 0.05% Tween-20 three times, the membranes were incubated with anti-rabbit or anti-mouse secondary antibodies (horseradish peroxidase-conjugated) for 1h at room temperature. Protein-specific signals were then detected with enhanced chemiluminescence substrate (GE Healthcare, Chalfont, Buckinghamshire, UK) using a Chemi™Doc imaging system (Bio-Rad 215 Laboratories, Hercules, CA) and then quantified with the software of Image lab 5.2 (Bio-Rad Laboratories, Hercules, CA).

Immunohistochemistry and immunofluorescence

Mouse brains were dissected and processed for immunofluorescence (IF) or immunohistochemistry (IHC) staining as previously described (Chen *et al.* 2012; Ke *et al.* 2011). In brief, brain tissues were fixed with 4% paraformaldehyde (PFA) overnight and then transferred to 30% sucrose to dehydrate. Next, the brain tissues were sectioned sagittally at a thickness of 15 μm and then mounted onto superfrost/plus slides. The slides mounted with brain sections were incubated with 0.3% H_2O_2 in methanol, permeabilized with 1% Triton X-100 and blocked with 1% BSA at room temperature. After that, these slides were immunostained with the following individual or combined primary antibodies: MANF (1:200), cleaved caspase 3 (1:200), CHOP (1:50), or NeuN (1:200). The slides were then incubated with anti-rabbit or anti-mouse secondary antibody conjugated to Alexa Fluor 488 or biotin. The immunolabelings were visualized using nickel-enhanced 3,3'-Diaminobenzidine (DAB) or Alexa Fluor 488 (green) and imaged with an inverted fluorescent microscope (IX81, Olympus).

TUNEL assay

Brain sections were prepared and mounted to slides as described above and then subjected to TUNEL analysis according to the protocol from manufacture (Roche, Cat No. 11684817910). In brief, the brain sections/slides were incubated with a blocking solution (3% H_2O_2 in methanol) for 10 minutes and then incubated with permeabilization solution (0.1% Triton X-100 and 0.1% sodium citrate) for 2 minutes. Next, these sections/slides were incubated with TUNEL reaction mixture at 37°C in a humidified atmosphere in the dark for 60 minutes. A brain section incubated with labeling solution was used as the negative control and a brain section digested with DNase I and incubated with TUNEL reaction mixture as the positive control. The slides were then mounted with DAPI-containing medium and imaged with an inverted fluorescent microscope (IX81, Olympus).

RNA isolation and real-time PCR

Total RNA from the brain or liver was extracted using Trizol Reagent (Life Technologies) and treated with RNA-free DNAase I to remove remnant DNA as described previously (Kim *et al.* 2014). cDNA used for gene detection was synthesized as described previously using

SuperScript III reverse transcriptase and random primers (Kim *et al*. 2014). The primers used for this study were purchased from Fisher Scientific as below: *UBXN6*, Mm01272178; *GRP78*, Mm00517691; *UBE2J2*, Mm01263784; *PDIA6*, Mm01270904; *ERLEC1*, Mm00458735; *HYOU1*, Mm00491279; *Manf*, Mm00512511; *18s rRNA*, Mm03928990. The relative expression was normalized to internal control (*18s rRNA*) using cycle time (Ct). The relative difference between the control and treatment group was expressed and calculated as relative increases using $2^{-\Delta\Delta Ct}$ and setting control as 1.

RNA sequencing and data analysis

Total RNA was isolated from brain tissues of two groups of PD7 mice with each group having three samples: CTL group and cKO group. Therefore, six RNA samples were submitted to the University of Kentucky Genomics Core Laboratory for the whole transcriptome sequencing. Libraries were assembled using the KAPA RNA HyperPrep Kits with RiboErase (HMR) for Illumina Platforms and indexed with KAPA Single-Indexed Adapter Kit (KAPA Biosystems). Indexed libraries were pooled in equimolar concentrations and the denatured pool diluted to a final concentration of 10 pM. This pool was spiked with 5% PhiX Control library. The combined pool was clustered on board using a HiSeq SR Rapid Cluster Kit v2 (Illumina) and sequenced on an Illumina HiSeq 2500 Sequencing system using a HiSeq Rapid SBS Kit v2 (Illumina).

The transcriptome of each sample was analyzed with ensemble GRCm38 Mouse Transcriptome as reference. Transcript abundance was calculated with RNA-Seq by Expectation-Maximization (RSEM) analysis (Li & Dewey 2011) and differentially expressed genes were calculated using EBSeq (Leng *et al*. 2015). A false detection rate (FDR) analysis with a 0.05 threshold was performed. The lists of DE genes were submitted to Enrichr for gene ontology enrichment (GOEA) analysis (Kuleshov *et al*. 2016).

Statistics

The data were expressed as mean ± SEM, and statistical significance was determined using Student Unpaired t-test, one-way ANOVA, or two-way ANOVA followed by Bonferroni Multiple Comparison test (GraphPad Prism version 7). A p-value of less than 0.05 was considered statistically significant.

Results

Characterization of the CNS-specific *Manf* knockout mouse model

CNS-*Manf*-KO (cKO) mice exhibited a CNS-specific *Manf* knockout (Figure 2A). The expression level of MANF was dramatically decreased across the entire mouse brain compared with that in control (CTL) littermates (*Manf* $^{flox/flox}$ mice) (Figure 2A and 2B). We also measured the body weight and brain weight and calculated the ratio of brain weight to body weight in cKO mice and CTL littermates. In brevity, the weight of cKO mouse brain and body was less than that in the CTL group (Figure 2C and 2D). However, the ratio of brain weight to body weight between these two groups showed no significant difference (Figure 2E). It is noteworthy that the difference in body weight can extend to the adult stage (Figure 2F). We thought the decrease in body weight and brain weight might be due to the

involvement of MANF in neuronal development and energy metabolism. Consistent with the previous report, we did not observe significant behavioral changes in cKO mice (Pakarinen *et al.* 2020a). However, some Manf KO dams did not take care of their pups as well as wild-type dams, and foster dams were sometimes necessary.

MANF deficiency alters ER-related RNA signature and causes ER stress in the developing mouse brain

To investigate whether MANF is involved in ER stress regulation, we conducted RNA-Seq and examined RNA expression profile in ER using brain samples from the CTL and cKO groups. A total of 2212 differentially expressed (DE) genes were detected (not shown here); however, only 933 had identified identifiers (not shown here). The 933 genes were associated with many signaling pathways and a total of 18 DE genes were identified to be associated with protein assessing in the endoplasmic reticulum (Table 1). Among these 18 genes, most of them were upregulated by *Manf* cKO; three genes (EDEM3, UBE2J2, and UBXN6) were downregulated in the brain of *Manf* cKO mice (Table 1 and Figure 3A). In term of gene function, eight genes (PDIA3, GRP78, PDIA6, DDOST, PDIA4, HSP90B1, DNAJC3, and HYOU1) were associated with protein chaperoning function or protein folding, seven genes (EDEM3, UBE2J2, ERLEC1, SELENOS, UGGT1, UBXN6, and ATF4) were associated with protein quality control or ER-associated degradation, whereas three genes (RRBP1, SEC61A1, and SEC24D) were mainly involved in protein trafficking or secretory pathways. We verified those DE genes that showed more than 1.5 folds change between the CTL group and the cKO group by RT-qPCR (Figure 3B–H). As expected, *Manf* mRNA level was significantly reduced in the brain of *Manf* cKO mice (Figure 3B). Overall, the results were consistent with our RNA-Seq data, reflecting the same change of those targets in the *Manf* cKO group (Figure 3C, 3D, 3G and 3H). However, we did find that the expression level of GRP78 and ERLEC1 did not differ significantly between the control group and *Manf* cKO group (Figure 3E and 3F). In summary, the RNA-Seq results further demonstrated that MANF acted as an ER stress-buffering agent and that MANF deficiency caused dysregulation of genes associated with protein folding.

There was no significant induction of neuronal apoptosis (Figure 4A and 4B) in the cKO mouse brain. However, MANF deficiency caused a modest increase in ER stress manifested by the upregulation of GRP78 and ATF6 (Figure 4C). This finding is consistent with the recent report showing that MANF ablation causes prolonged activation of the UPR with the absence of neurodegeneration in the mouse brain (Pakarinen *et al.* 2020b).

MANF deficiency exacerbates ethanol- and TM-induced neuronal apoptosis in the developing brain

To investigate the effects of MANF deficiency on ethanol-induced neuronal apoptosis, a modified neonatal ethanol exposure paradigm was employed (Olney *et al.* 2002). This ethanol exposure paradigm resulted in a BEC of 185 ± 10 mg/dl. The BEC was similar between CTL and cKO mice (data not shown). While ethanol exposure alone resulted in moderate neuronal apoptosis in the developing mouse brain, we found that MANF deficiency dramatically promoted ethanol neurotoxicity (Figure 5A and 2B). Co-labelling with TUNEL and NeuN (a neuron marker) revealed that almost all of the apoptotic cells

were neurons (Figure 5C). The apoptotic neurons, in general, spread across the entire brain, but some regions (e.g., frontal cortex, cerebellum, thalamus, and hippocampus), indeed, showed more vulnerability. To investigate whether the effects of MANF are ubiquitous to all ER stress-characterized neurodegenerative diseases, we treated the mice with a general ER stress inducer, TM (3 mg/kg, 30% solution in dextrose) following the same procedure except that the treatment duration was 24 hours. The results presented a similar pattern showing that MANF deficiency exacerbated TM-induced neuronal apoptosis, especially in the frontal cortex, cerebellum, and hippocampus (Figure 5D and 5E). Taken together, these results suggest that MANF is neuroprotective against ethanol-induced neuronal apoptosis and that the neuroprotective effects of MANF likely apply to ER stress-characterized neurodegenerative diseases.

MANF deficiency promotes ethanol- and TM-induced ER stress in the developing mouse brain

To determine whether the resulting increase of neuronal apoptosis was attributed to ER stress over-activation, we examined ER stress levels in the entire mouse brain and compared that level between CTL pups and cKO pups following the same treatment and procedure. Consistent with our published results, we found a moderate increase in ER stress due to ethanol or TM exposure alone (Figure 6A and 6D). However, we found MANF deficiency potentiated ethanol- or TM-induced ER stress, causing a further dramatic enhancement of ER stress in the cerebral cortex, cerebellum, and hippocampus of the mouse brain (Figure 6A–E). This data suggests that MANF may function as an ER stress-buffering agent, and the deficiency of MANF exacerbates ethanol- or TM-induced ER stress. Notably, while ethanol- or TM-induced apoptosis is more confined to specific brain regions, e.g., cerebellum, cerebral cortex, or hippocampus, the induction of ER stress is more wide-spread.

Blocking ER stress abrogates MANF deficiency-induced exacerbation of neuronal apoptosis

Co-labeling with TUNEL and CHOP (an ER stress marker) revealed that most apoptotic neurons expressed a high level of CHOP, indicating that neuronal apoptosis might be associated with the induction of ER stress (Figure 6C). To determine whether the increase of neuronal apoptosis due to MANF deficiency was attributed to the exacerbation of ER stress, we have employed a pharmacological inhibitor of ER stress–4-PBA. 4-PBA is a chemical chaperone that has been widely used to prevent ER stress in the liver, adipose tissue, and brain. 4-PBA did not significantly change BEC (data not shown). In our animal models, pretreatment with 4-PBA can block ethanol- and TM-induced ER stress both in the CTL group and cKO mice (Figure 7A and 7C). Meanwhile, ethanol- and TM- induced neuronal apoptosis was also abolished by the employment of 4-PBA (Figure 7A–D). Collectively, this data suggests that the overactivation of ER stress is accountable for the exacerbation of neuronal apoptosis.

Discussion

We demonstrate that MANF is neuroprotective against ethanol-induced neurodegeneration through ameliorating ER stress and the neuroprotective role of MANF is likely applied to

other ER stress-characterized neurodegenerative diseases. Moreover, the results from a whole transcriptome RNA sequencing on brain samples from *Manf* cKO mice and control mice provide evidence about the involvement of MANF in ER stress regulation and shed light on the potential targets that mediate the ER stress-buffering capacity of MANF in ethanol-induced neurodegeneration.

A third-trimester equivalent mouse model is used in our study to model developmental exposure to ethanol. Due to a developmental timing shift between humans and rodents, the developmental period of the rodent brain in PD1–10 is equivalent to the third trimester in humans when brain growth spurt occurs (Semple *et al.* 2013). The original model was established by Olney's group and was widely used to induce neurodegeneration in infant mice (Olney *et al.* 2002). In addition, we choose to examine the impact of MANF on ethanol- and TM-induced ER stress and neuronal death in the developing mouse brain for the following two reasons. First, ER stress is responsive to ethanol exposure in the developing brain to a greater extent than in the adult brain (Ke *et al.* 2011; Wang *et al.* 2018). Second, the expression level of MANF varies over time during brain development; it has its highest expression during the developmental stage and declines afterward (Wang *et al.* 2014). We believe that the beneficial effects of MANF on ER stress and ethanol- and TM-induced neurodegeneration is more predominant in the developing brain than in the adult brain.

MANF ablation alone does not result in neurodegeneration, but causes a modest activation of UPR. This finding is consistent with the recently published results, suggesting that MANF deficiency alone is not sufficient to elicit the pathological phenotype-neurodegeneration (Pakarinen *et al.* 2020b). Next, we investigate the effects of MANF on ER stress and neurodegeneration in pathological conditions: ethanol- and TM-induced neurodegeneration. MANF deficiency exacerbates ethanol- and TM-induced ER stress and neurodegeneration. The results suggest that the beneficial effects of MANF may be ubiquitous to all ER stress-characterized neurodegenerative diseases. Nevertheless, brain regions that are sensitive to these two respective inducements vary. Neuronal apoptosis in the TM-induced neurodegenerative model mainly occurs in the cerebellum, whereas the apoptotic cells in the ethanol-induced neurodegenerative model are wide-spread, with some regions appearing more vulnerable, such as the frontal cortex, cerebellum, thalamus, and hippocampus.

MANF expression is generally regulated by the transcriptional activation of ATF6 and XBP1s through the binding of the ER stress response element II (ERSE-II) and ERSE-I located in its promotor region, respectively (Oh-Hashi, Hirata, & Kiuchi, 2013; D. Wang et al., 2018; Tadimalla *et al.* 2008). Our result shows that ethanol- and TM-exposure caused a significant upregulation of both ATF6 and XBP1s proteins (Figs 6 and 7), suggesting that ethanol may increase MANF expression by targeting ATF6 and XBP1s. Although MANF is an ER-resident protein, secretory MANF has been found in circulation and interstitial tissue (Lindholm & Saarma 2010). ER stress can stimulate a robust secretion of MANF (Henderson, Richie, Airavaara, Wang, & Harvey, 2013). Both intracellular and extracellular MANF exhibits protective effects in different disease models. Injection of recombinant MANF protein into brain regions were reported to alleviate ER stress and protect neurons in

cerebral ischemia and animal models of Parkinson's disease (Voutilainen et al., 2009; W. Yang et al., 2014). *In vitro* studies using cultured neuronal cells have also demenstrated a protective effect of extracellular MANF in Alzheimer's disease and Parkinson's disease models (Liu et al., 2018; S. Xu et al., 2019). Our results indicate that MANF functions as an ER stress-buffering agent to ameliorate ER stress and as a result, MANF deficiency causes a deterioration of ER stress. While the exact mechanisms that underlie the buffering effects of MANF on ER stress remain unclear, several mechanisms have been proposed. A study recently reported that the SAP domain of MANF interacts with BiP, antagonizing BiP-mediated nucleotide change, and thereby stabilizes BiP-client complexes to facilitate protein folding (Yan *et al.* 2019). Second, MANF contains a C-XX-C motif and has been reported to be involved in disulfide bond formation, a critical step in protein folding in the ER (Hoseki *et al.* 2010). Alternatively, one group demonstrated that MANF is a structurally unique redox-sensitive chaperone that can restore protein folding in the ischemic heart (Arrieta *et al.* 2017).

Our RNA sequencing data confirm the functionality of MANF in ER stress regulation. In addition to the ER stress markers that are confirmed by immunoblots, it has identified a number of targets that are ER-resident protein responsible for the folding and trafficking of newly synthesized protein. These target proteins carry on a series of functions ranging from protein chaperoning, protein disulfide isomerization to ER-associated protein degradation. It should be noted that these proteins could be direct targets of MANF or indirect targets that are indicative of the deterioration of ER stress. Most of the upregulated transcripts are ER-resident chaperones or protein disulfides (PDIs) that can improve an adaptation to ER stress, whereas most of the downregulated transcripts (UBE2J2 and UBXN6) are ubiquitin-conjugating enzymes that are involved in proteasomal degradation (Nagahama *et al.* 2009; Wang *et al.* 2009). We speculate that MANF deficiency may disrupt the ubiquitination system and consequently causes ER stress manifested by an abrupt increase of ER stress-related transcripts. Further experiments are needed to identify their physical and functional connection with MANF.

In summary, we have established a CNS-specifc *Manf* knockout mouse model and provided strong evidence using this model of loss-of-function of MANF, that MANF is neuroprotective against ethanol or TM-induced neurodegeneration in the developing brain through ameliorating ER stress. Additional research would strength the current study. First, the direct evidence regarding the effects of gain-of-function of MANF on ethanol- or TM-induced ER stress and neurodegeneration would further verify the current findings. Second, although MANF is an ER-resident protein, it is also a secretory factor, typically in stressful conditions (Henderson *et al.* 2013). A study designed to delineate the contribution of intracellular MANF or extracellular MANF on ethanol-induced neuroprotection would be worthwhile. Lastly, MANF is expressed in both neurons and glial cells (Lindholm *et al.* 2008). It would be interesting to differentiate the contribution of neuron- or astrocyte-derived MANF to its protection against ethanol-induced neuronal damage. A better understanding of the role of MANF in ethanol-induced neurodegeneration may reveal MANF as a critical player in ER stress regulation, thereby laying a foundation for targeting MANF as a therapeutic approach in the treatment of FASD.

Acknowledgments and conflict of interest disclosure

We thank Dr. Chi Wang and Daheng He for providing Gene Ontology (GO) analysis. This work is supported by grants from the National Institute of Health (NIH) (AA017226 and AA015407) and NIH training grant (T32 DK007778). It is also supported in part by the Department of Veterans Affairs, Veterans Health Administration, Office of Research and Development [Biomedical Laboratory Research and Development: Merit review (BX001721)]. The authors declare no conflicts of interest.

Abbreviation used:

ATF6	activating transcription factor 6
ARMET	arginine-rich mutated in early stages of tumor
AUD	alcohol use disorder
BBB	blood-brain barrier
BEC	blood ethanol concentration
CHOP	CCAAT/enhancer-binding protein homologous protein
CNS	central nervous system
DAMP	damage-associated molecular pattern
ER	endoplasmic reticulum
FASD	fetal alcohol spectrum disorders
HMGB1	high mobility group box 1
IRE1	Inositol-requiring kinase
MANF	mesencephalic astrocyte-derived neurotrophic factor
NF-κβ	nuclear factor kappa-light-chain-enhancer of activated B cells
4-PBA	sodium phenylbutyrate
PD	postnatal day
PERK	protein kinase RNA-like endoplasmic reticulum kinase
RAGE	receptor for advanced glycation end products
TLR	toll-like receptors
TM	tunicamycin
TNFα	tumor necrosis factor-alpha
UPR	unfolded protein response

References

Aguzzi A and O'Connor T (2010) Protein aggregation diseases: pathogenicity and therapeutic perspectives. Nat Rev Drug Discov 9, 237–248. [PubMed: 20190788]

Apostolou A, Shen Y, Liang Y, Luo J and Fang S (2008) Armet, a UPR-upregulated protein, inhibits cell proliferation and ER stress-induced cell death. Exp Cell Res 314, 2454–2467. [PubMed: 18561914]

Arrieta A, Blackwood E, Stauffer WT, Domingo MS, Pentoney AN, Thuerauf DJ, Doroudgar S and Glembotski CC (2017) MANF, a structurally unique redox-sensitive chaperone, restores ER-protein folding in the ischemic heart. Journal of Molecular and Cellular Cardiology 112, 165.

Chen G, Ke Z, Xu M et al. (2012) Autophagy is a protective response to ethanol neurotoxicity. Autophagy 8, 1577–1589. [PubMed: 22874567]

Connor PD, Sampson PD, Streissguth AP, Bookstein FL and Barr HM (2006) Effects of prenatal alcohol exposure on fine motor coordination and balance: A study of two adult samples. Neuropsychologia 44, 744–751. [PubMed: 16154165]

Crews FT and Nixon K (2009) Mechanisms of neurodegeneration and regeneration in alcoholism. Alcohol Alcohol 44, 115–127. [PubMed: 18940959]

Crews FT and Vetreno RP (2016) Mechanisms of neuroimmune gene induction in alcoholism. Psychopharmacology (Berl) 233, 1543–1557. [PubMed: 25787746]

Dara L, Ji C and Kaplowitz N (2011) The contribution of endoplasmic reticulum stress to liver diseases. Hepatology 53, 1752–1763. [PubMed: 21384408]

Diwadkar VA, Meintjes EM, Goradia D, Dodge NC, Warton C, Molteno CD, Jacobson SW and Jacobson JL (2013) Differences in cortico-striatal-cerebellar activation during working memory in syndromal and nonsyndromal children with prenatal alcohol exposure. Hum Brain Mapp 34, 1931–1945. [PubMed: 22451272]

Ferrier L, Berard F, Debrauwer L, Chabo C, Langella P, Bueno L and Fioramonti J (2006) Impairment of the intestinal barrier by ethanol involves enteric microflora and mast cell activation in rodents. Am J Pathol 168, 1148–1154. [PubMed: 16565490]

Glass L, Ware AL and Mattson SN (2014) Neurobehavioral, neurologic, and neuroimaging characteristics of fetal alcohol spectrum disorders. Handb Clin Neurol 125, 435–462. [PubMed: 25307589]

Hellman M, Arumae U, Yu LY, Lindholm P, Peranen J, Saarma M and Permi P (2011) Mesencephalic astrocyte-derived neurotrophic factor (MANF) has a unique mechanism to rescue apoptotic neurons. J Biol Chem 286, 2675–2680. [PubMed: 21047780]

Henderson MJ, Richie CT, Airavaara M, Wang Y and Harvey BK (2013) Mesencephalic astrocyte-derived neurotrophic factor (MANF) secretion and cell surface binding are modulated by KDEL receptors. J Biol Chem 288, 4209–4225. [PubMed: 23255601]

Hetz C and Saxena S (2017) ER stress and the unfolded protein response in neurodegeneration. Nat Rev Neurol 13, 477–491. [PubMed: 28731040]

Hoseki J, Sasakawa H, Yamaguchi Y, Maeda M, Kubota H, Kato K and Nagata K (2010) Solution structure and dynamics of mouse ARMET. FEBS Lett 584, 1536–1542. [PubMed: 20214902]

Ji C and Kaplowitz N (2006) ER stress: can the liver cope? J Hepatol 45, 321–333. [PubMed: 16797772]

Ji C, Kaplowitz N, Lau MY, Kao E, Petrovic LM and Lee AS (2011) Liver-specific loss of glucose-regulated protein 78 perturbs the unfolded protein response and exacerbates a spectrum of liver diseases in mice. Hepatology 54, 229–239. [PubMed: 21503947]

Ji C, Mehrian-Shai R, Chan C, Hsu YH and Kaplowitz N (2005) Role of CHOP in hepatic apoptosis in the murine model of intragastric ethanol feeding. Alcohol Clin Exp Res 29, 1496–1503. [PubMed: 16131858]

Joseph J, Warton C, Jacobson SW et al. (2014) Three-dimensional surface deformation-based shape analysis of hippocampus and caudate nucleus in children with fetal alcohol spectrum disorders. Hum Brain Mapp 35, 659–672. [PubMed: 23124690]

Kane CJM and Drew PD (2020) Neuroinflammatory contribution of microglia and astrocytes in fetal alcohol spectrum disorders. J Neurosci Res.

Ke Z, Wang X, Liu Y et al. (2011) Ethanol induces endoplasmic reticulum stress in the developing brain. Alcohol Clin Exp Res 35, 1574–1583. [PubMed: 21599712]

Kim IM, Wang Y, Park KM et al. (2014) beta-arrestin1-biased beta1-adrenergic receptor signaling regulates microRNA processing. Circ Res 114, 833–844. [PubMed: 24334028]

Kratsovnik E, Bromberg Y, Sperling O and Zoref-Shani E (2005) Oxidative stress activates transcription factor NF-kB-mediated protective signaling in primary rat neuronal cultures. J Mol Neurosci 26, 27–32. [PubMed: 15968083]

Kubisch CH, Sans MD, Arumugam T, Ernst SA, Williams JA and Logsdon CD (2006) Early activation of endoplasmic reticulum stress is associated with arginine-induced acute pancreatitis. Am J Physiol Gastrointest Liver Physiol 291, G238–245. [PubMed: 16574987]

Kuleshov MV, Jones MR, Rouillard AD et al. (2016) Enrichr: a comprehensive gene set enrichment analysis web server 2016 update. Nucleic Acids Res 44, W90–97. [PubMed: 27141961]

Lebel C, Roussotte F and Sowell ER (2011) Imaging the impact of prenatal alcohol exposure on the structure of the developing human brain. Neuropsychol Rev 21, 102–118. [PubMed: 21369875]

Leng N, Li Y, McIntosh BE et al. (2015) EBSeq-HMM: a Bayesian approach for identifying gene-expression changes in ordered RNA-seq experiments. Bioinformatics 31, 2614–2622. [PubMed: 25847007]

Li B and Dewey CN (2011) RSEM: accurate transcript quantification from RNA-Seq data with or without a reference genome. BMC Bioinformatics 12, 323. [PubMed: 21816040]

Li H, Wen W, Xu H, Wu H, Xu M, Frank JA and Luo J (2019) 4-Phenylbutyric Acid Protects Against Ethanol-Induced Damage in the Developing Mouse Brain. Alcohol Clin Exp Res 43, 69–78. [PubMed: 30403409]

Li SY and Ren J (2008) Cardiac overexpression of alcohol dehydrogenase exacerbates chronic ethanol ingestion-induced myocardial dysfunction and hypertrophy: role of insulin signaling and ER stress. J Mol Cell Cardiol 44, 992–1001. [PubMed: 18377926]

Lindholm P, Peranen J, Andressoo JO, Kalkkinen N, Kokaia Z, Lindvall O, Timmusk T and Saarma M (2008) MANF is widely expressed in mammalian tissues and differently regulated after ischemic and epileptic insults in rodent brain. Mol Cell Neurosci 39, 356–371. [PubMed: 18718866]

Lindholm P and Saarma M (2010) Novel CDNF/MANF family of neurotrophic factors. Dev Neurobiol 70, 360–371. [PubMed: 20186704]

Lucas SM, Rothwell NJ and Gibson RM (2006) The role of inflammation in CNS injury and disease. Br J Pharmacol 147 Suppl 1, S232–240. [PubMed: 16402109]

Lugea A, Tischler D, Nguyen J, Gong J, Gukovsky I, French SW, Gorelick FS and Pandol SJ (2011) Adaptive unfolded protein response attenuates alcohol-induced pancreatic damage. Gastroenterology 140, 987–997. [PubMed: 21111739]

Marciniak SJ and Ron D (2006) Endoplasmic reticulum stress signaling in disease. Physiol Rev 86, 1133–1149. [PubMed: 17015486]

Mattson SN, Crocker N and Nguyen TT (2011) Fetal alcohol spectrum disorders: neuropsychological and behavioral features. Neuropsychol Rev 21, 81–101. [PubMed: 21503685]

Mattson SN, Roesch SC, Glass L et al. (2013) Further development of a neurobehavioral profile of fetal alcohol spectrum disorders. Alcohol Clin Exp Res 37, 517–528. [PubMed: 22974253]

May PA, Chambers CD, Kalberg WO et al. (2018) Prevalence of Fetal Alcohol Spectrum Disorders in 4 US Communities. JAMA 319, 474–482. [PubMed: 29411031]

Morgan MJ and Liu ZG (2011) Crosstalk of reactive oxygen species and NF-kappaB signaling. Cell Res 21, 103–115. [PubMed: 21187859]

Nagahama M, Ohnishi M, Kawate Y, Matsui T, Miyake H, Yuasa K, Tani K, Tagaya M and Tsuji A (2009) UBXD1 is a VCP-interacting protein that is involved in ER-associated degradation. Biochem Biophys Res Commun 382, 303–308. [PubMed: 19275885]

Neves J, Zhu J, Sousa-Victor P, Konjikusic M, Riley R, Chew S, Qi Y, Jasper H and Lamba DA (2016) Immune modulation by MANF promotes tissue repair and regenerative success in the retina. Science 353, aaf3646. [PubMed: 27365452]

Norman AL, Crocker N, Mattson SN and Riley EP (2009) Neuroimaging and fetal alcohol spectrum disorders. Dev Disabil Res Rev 15, 209–217. [PubMed: 19731391]

Olney JW, Tenkova T, Dikranian K, Qin YQ, Labruyere J and Ikonomidou C (2002) Ethanol-induced apoptotic neurodegeneration in the developing C57BL/6 mouse brain. Brain Res Dev Brain Res 133, 115–126. [PubMed: 11882342]

Pakarinen E, Danilova T, Voikar V, Chmielarz P, Piepponen P, Airavaara M, Saarma M and Lindahl M (2020a) MANF Ablation Causes Prolonged Activation of the UPR without Neurodegeneration in the Mouse Midbrain Dopamine System. eNeuro 7.

Pakarinen E, Danilova T, Voikar V, Chmielarz P, Piepponen P, Airavaara M, Saarma M and Lindahl M (2020b) MANF ablation causes prolonged activation of the UPR without neurodegeneration in the mouse midbrain dopamine system. eNeuro.

Pandol SJ, Gorelick FS, Gerloff A and Lugea A (2010) Alcohol abuse, endoplasmic reticulum stress and pancreatitis. Dig Dis 28, 776–782. [PubMed: 21525762]

Patten AR, Fontaine CJ and Christie BR (2014) A comparison of the different animal models of fetal alcohol spectrum disorders and their use in studying complex behaviors. Front Pediatr 2, 93. [PubMed: 25232537]

Petrova P, Raibekas A, Pevsner J et al. (2003) MANF: a new mesencephalic, astrocyte-derived neurotrophic factor with selectivity for dopaminergic neurons. J Mol Neurosci 20, 173–188. [PubMed: 12794311]

Qin L and Crews FT (2012) NADPH oxidase and reactive oxygen species contribute to alcohol-induced microglial activation and neurodegeneration. J Neuroinflammation 9, 5. [PubMed: 22240163]

Qin L, He J, Hanes RN, Pluzarev O, Hong JS and Crews FT (2008) Increased systemic and brain cytokine production and neuroinflammation by endotoxin following ethanol treatment. J Neuroinflammation 5, 10. [PubMed: 18348728]

Ron D (2002) Translational control in the endoplasmic reticulum stress response. J Clin Invest 110, 1383–1388. [PubMed: 12438433]

Semple BD, Blomgren K, Gimlin K, Ferriero DM and Noble-Haeusslein LJ (2013) Brain development in rodents and humans: Identifying benchmarks of maturation and vulnerability to injury across species. Prog Neurobiol 106–107, 1–16.

Tadimalla A, Belmont PJ, Thuerauf DJ, Glassy MS, Martindale JJ, Gude N, Sussman MA and Glembotski CC (2008) Mesencephalic astrocyte-derived neurotrophic factor is an ischemia-inducible secreted endoplasmic reticulum stress response protein in the heart. Circ Res 103, 1249–1258. [PubMed: 18927462]

Tseng KY, Danilova T, Domanskyi A, Saarma M, Lindahl M and Airavaara M (2017) MANF Is Essential for Neurite Extension and Neuronal Migration in the Developing Cortex. eNeuro 4.

Voutilainen MH, Back S, Porsti E, Toppinen L, Lindgren L, Lindholm P, Peranen J, Saarma M and Tuominen RK (2009) Mesencephalic astrocyte-derived neurotrophic factor is neurorestorative in rat model of Parkinson's disease. J Neurosci 29, 9651–9659. [PubMed: 19641128]

Wang H, Ke Z, Alimov A, Xu M, Frank JA, Fang S and Luo J (2014) Spatiotemporal expression of MANF in the developing rat brain. PLoS One 9, e90433. [PubMed: 24587361]

Wang X, Herr RA, Rabelink M, Hoeben RC, Wiertz EJ and Hansen TH (2009) Ube2j2 ubiquitinates hydroxylated amino acids on ER-associated degradation substrates. J Cell Biol 187, 655–668. [PubMed: 19951915]

Wang Y, Wang X, Li H, Xu M, Frank J and Luo J (2018) Binge ethanol exposure induces endoplasmic reticulum stress in the brain of adult mice. Toxicol Appl Pharmacol 356, 172–181. [PubMed: 30114398]

Xu M, Wang S, Qi Y, Chen L, Frank JA, Yang XH, Zhang Z, Shi X and Luo J (2016) Role of MCP-1 in alcohol-induced aggressiveness of colorectal cancer cells. Mol Carcinog 55, 1002–1011. [PubMed: 26014148]

Yan Y, Rato C, Rohland L, Preissler S and Ron D (2019) MANF antagonizes nucleotide exchange by the endoplasmic reticulum chaperone BiP. Nat Commun 10, 541. [PubMed: 30710085]

Yang S, Yang H, Chang R et al. (2017) MANF regulates hypothalamic control of food intake and body weight. Nat Commun 8, 579. [PubMed: 28924165]

Yu YQ, Liu LC, Wang FC et al. (2010) Induction profile of MANF/ARMET by cerebral ischemia and its implication for neuron protection. J Cereb Blood Flow Metab 30, 79–91. [PubMed: 19773801]

Highlights

- Conditional MANF knockout in the central nervous system (CNS) alters endoplasmic reticulum (ER)-related RNA signature in the developing mouse brain.
- The ablation of MANF in CNS exacerbates ethanol- and tunicamycin (TM)-induced ER stress and neuronal apoptosis.
- ER stress plays an important role in MANF deficiency-promoted neuronal apoptosis in ethanol- and TM-exposed developing brain.

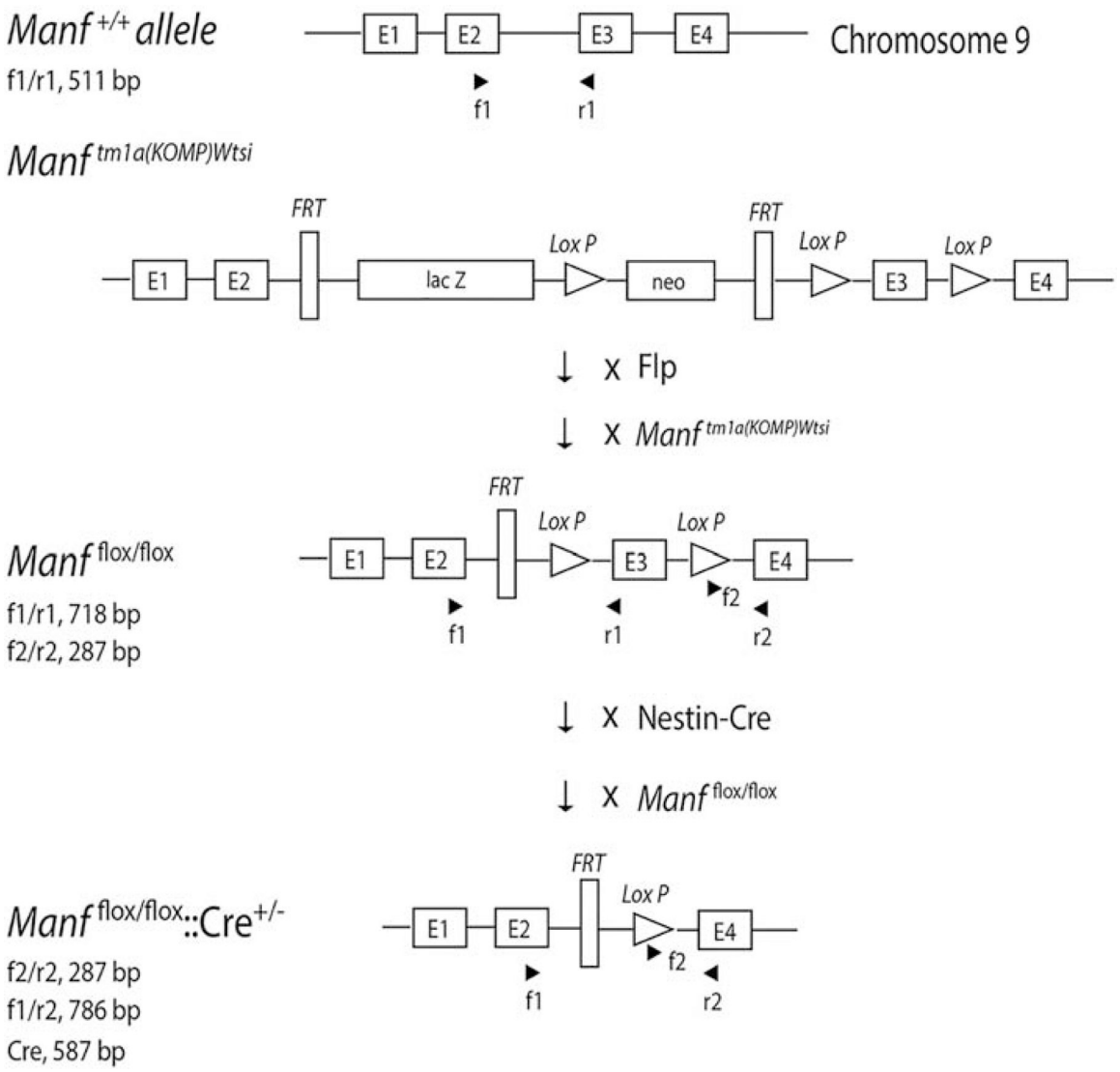

Figure 1. Schematic illustration of CNS-specific *Manf* knockout.

Schematic representation of *Manf*$^{+/+}$ wild-type, *Manf*$^{flox/flox}$, and *Manf*$^{flox/flox}$::Cre$^{+/-}$ targeted locus. E: exon. Arrowheads indicate priming sites used in genotyping by PCR.

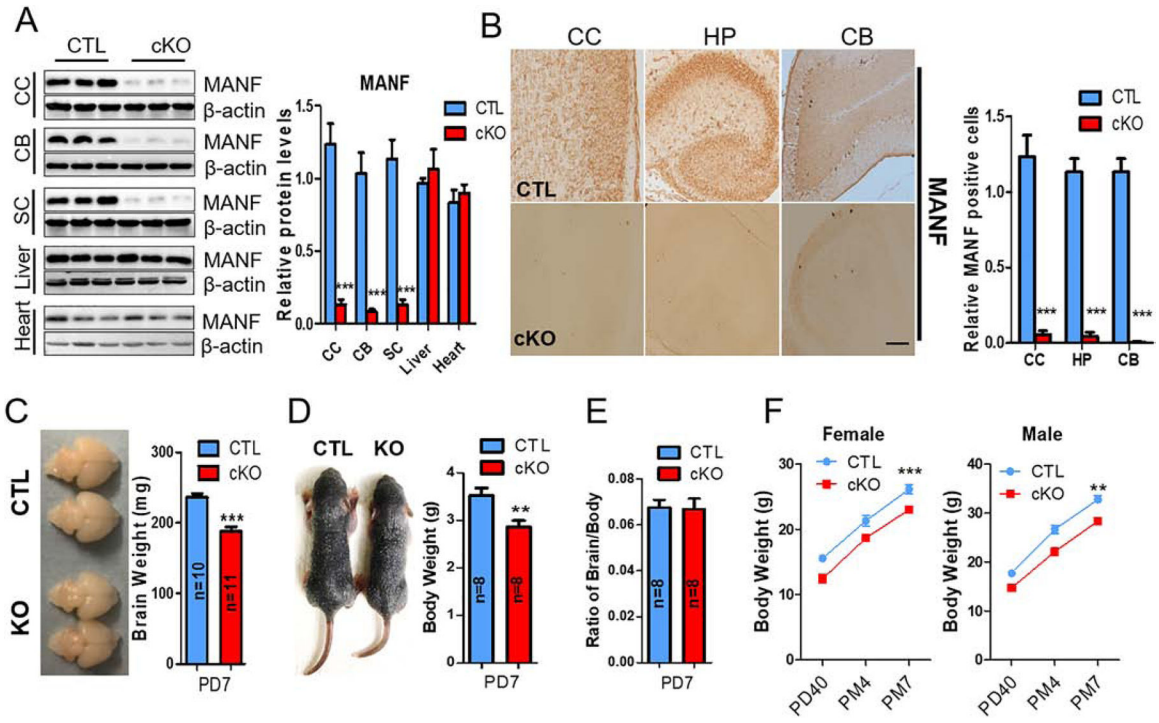

Figure 2. Characterization of the CNS-specific *Manf* knockout mouse model.

A. Representative immunoblots of MANF in cerebral cortex (CC), cerebellum (CB), subcortical structure (SC), liver and heart in the control (CTL) and *Manf* conditional knockout (cKO) mice. The data was expressed as mean ± SEM. n=3–5 per group, ***p<0.001 vs. CTL. **B**. Representative immunohistochemical staining of MANF in CC, HP (hippocampus) and CB sections of PD7 pups from the CTL and cKO groups. Scale bar: 20 um. n=3–5 animals per group, ***p<0.001 vs. CTL. **C-F**. Measurement and calculation of brain weight (**C**) and body weight (**D** and **F**) and the ratio of brain weight to body weight (E) in the CTL and cKO mice. PD: postnatal day. PM: postnatal month. n=8–11 per group, **p<0.01 or ***p<0.001 vs. CTL.

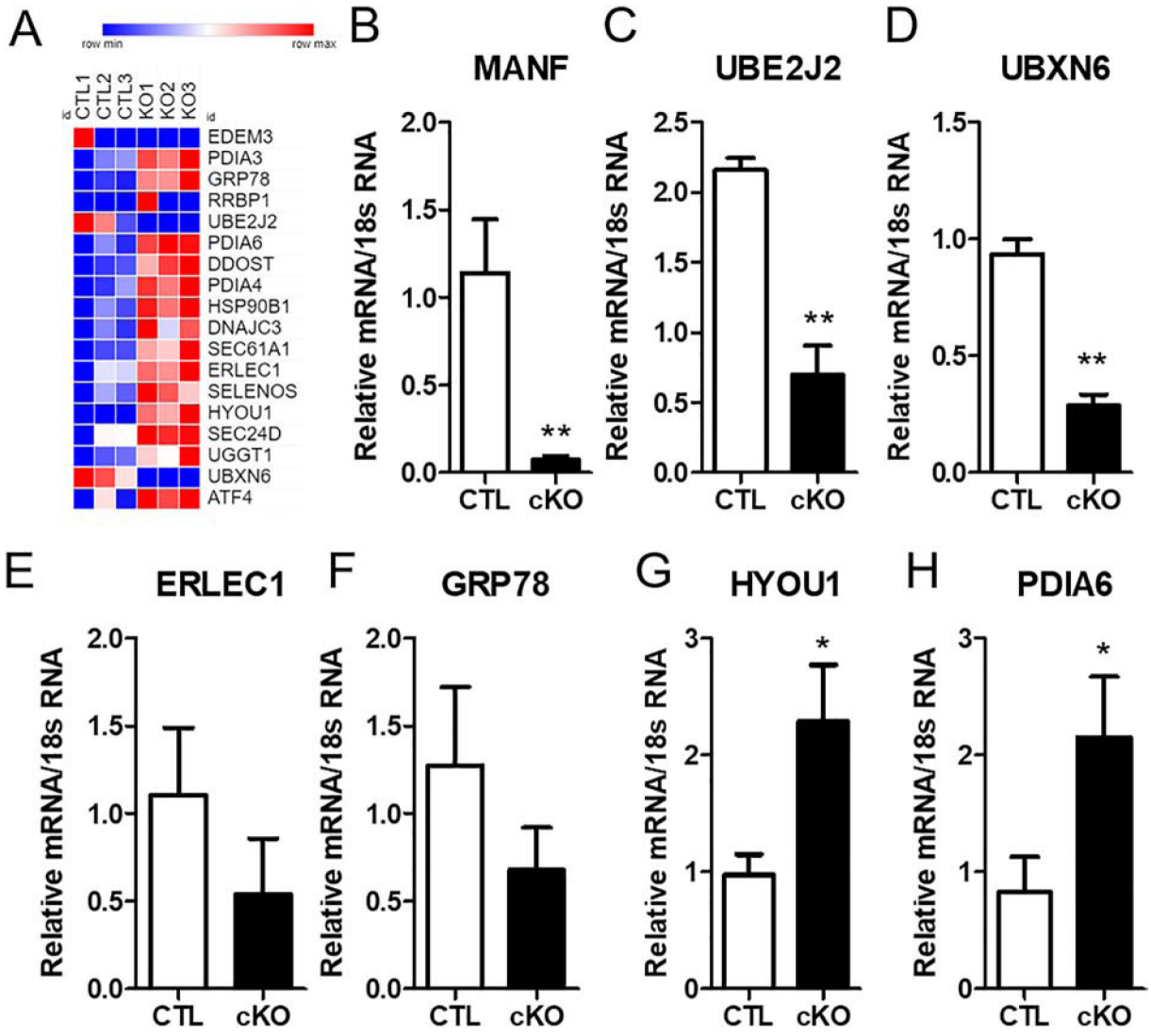

Figure 3. Verification of DE genes that are associated with protein processing in ER.

A. Heat map representing color-coded DE genes that are associated with protein processing in ER. **B-H**. Verification of DE genes that are associated with protein processing in ER by RT-qPCR. n=3, *p<0.05 or **p<0.01 vs. CTL.

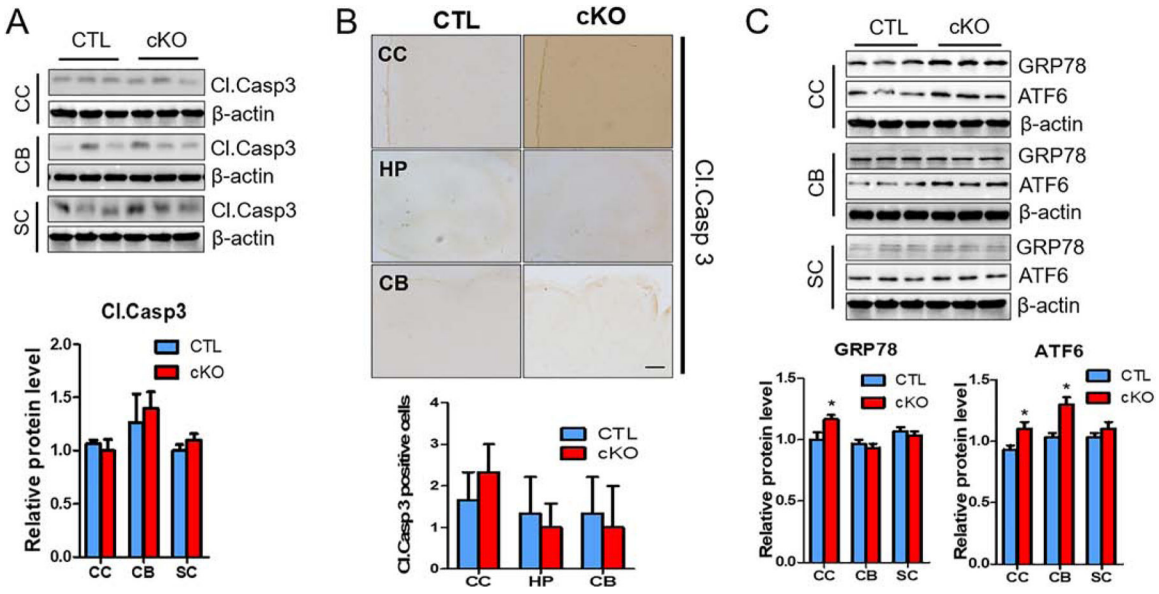

Figure 4. MANF deficiency causes ER stress in the developing mouse brain.

A. Representative immunoblots of cleaved caspase 3 (Cl. Casp 3) in cerebral cortex (CC), cerebellum (CB) and subcortical structure (SC) in the CTL and cKO mice. n=3–5. **B**. Representative immunohistochemical staining of Cl. Casp 3 in CC, HP (hippocampus) and CB sections of PD7 pups from the CTL and cKO groups. Scale bar: 20 um. n=3–5. **C.** Representative immunoblots of ER stress markers (GRP78 and ATF6) in cerebral cortex (CC), cerebellum (CB) and subcortical structure (SC) in the control (CTL) and *Manf* conditional knockout (cKO) mice. n=3–5, *p<0.05 vs. CTL.

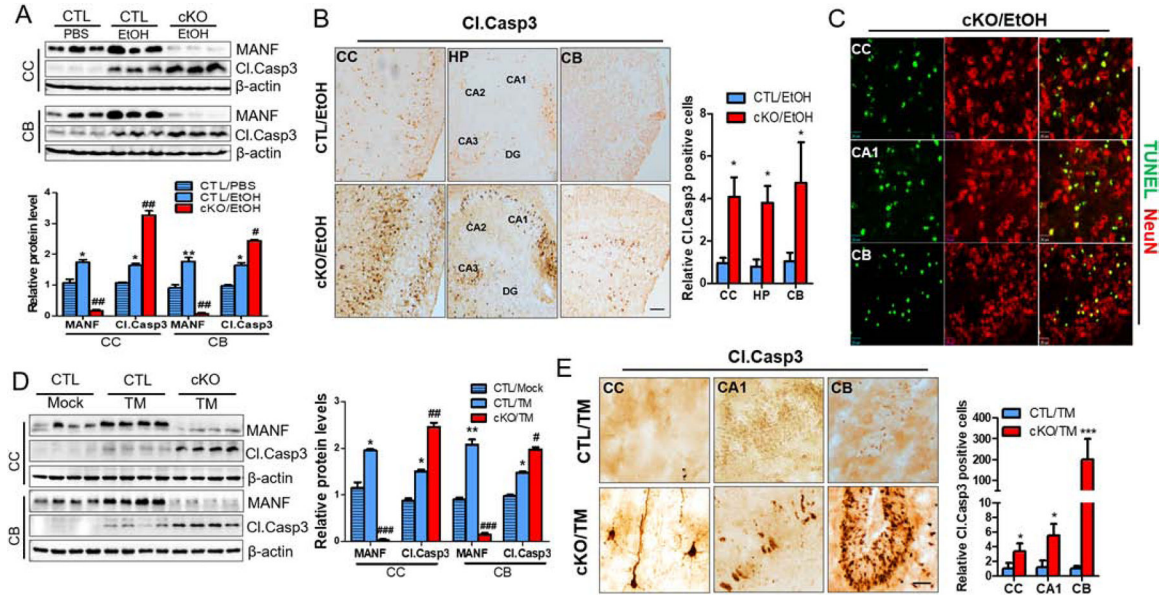

Figure 5. MANF deficiency exacerbates ethanol- and TM-induced neuronal apoptosis.

A. Representative immunoblots of MANF and cleaved caspase 3 (Cl.Casp3) in cerebral cortex (CC) and cerebellum (CB) of PD7 pups from the control (CTL/PBS and CTL/EtOH) and cKO (cKO/EtOH) groups. n=3–5, *p<0.05 or **p<0.01 vs. CTL/PBS. #p<0.05 or ##p<0.01 vs. CTL/EtOH. **B**. Representative immunohistochemical staining of Cl.Casp3 in CC, HP (hippocampus), and CB sections of PD7 pups from the control (CTL/EtOH) and cKO (cKO/EtOH) groups. Scale bar: 20 um. n=3–5, *p<0.05 vs. CTL/EtOH. **C**. Representative images of co-labeling with TUNEL (green) and NeuN (red) in CC, CA1, and CB sections of PD7 pups from the cKO group. Scale bar: 20um. **D**. Representative immunoblots of MANF and Cl. Casp3 in cerebral cortex (CC) and cerebellum (CB) of PD7 pups from the control (CTL/mock and CTL/TM) and cKO (cKO/TM) groups. n=3–5, *p<0.05 vs. CTL/mock. #p<0.05, ##p<0.01 or ###p<0.001 vs. CTL/TM. E. Representative staining of Cl.Casp3 in CC, CA1, and CB sections of PD7 pups from the control (CTL/TM) and cKO (cKO/TM) groups. Scale bar: 20 um. n=3–5, *p<0.05 or ***p<0.001 vs. CTL/TM.

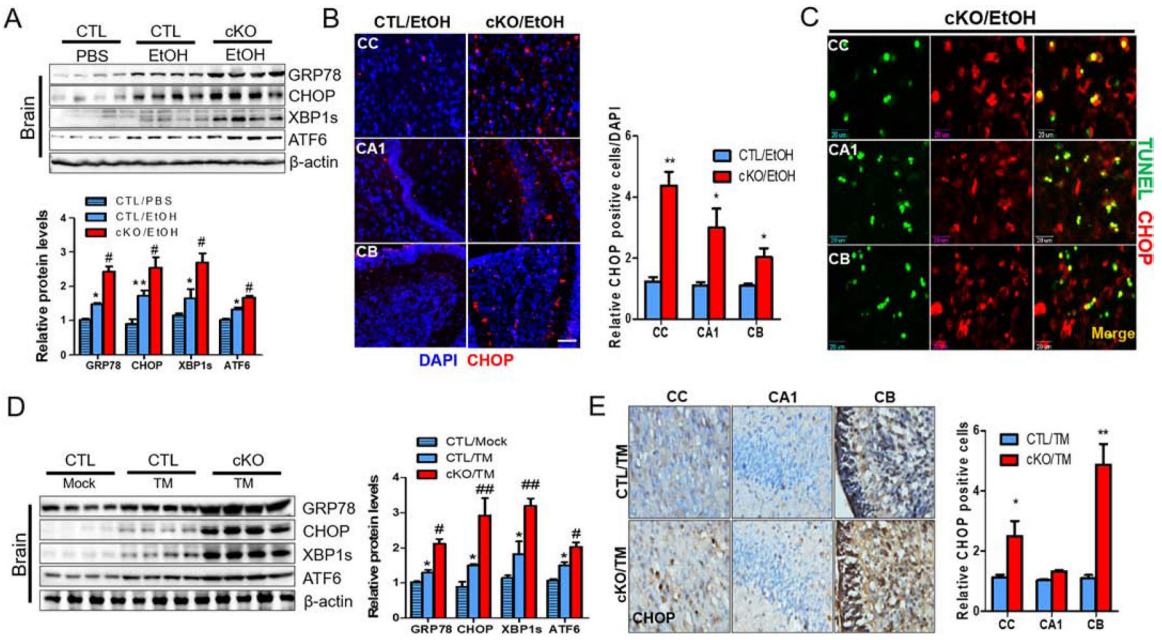

Figure 6. MANF deficiency exacerbates ethanol- and TM-induced ER stress.

A. Representative immunoblots of ER stress markers (GRP78, CHOP, XBP1s and ATF6) in the whole brains of PD7 pups from control (CTL/PBS and CTL/EtOH) and cKO (cKO/EtOH) groups. n=3–5, *p<0.05 or **p<0.01 vs. CTL/PBS. #p<0.05 vs. CTL/EtOH. **B**. Representative immunohistochemical staining of CHOP (red) and DAPI (blue) in CC, CA1, and CB sections of PD7 pups from control (CTL/EtOH) and cKO (KO/EtOH) groups. Scale bar: 20um. n=3–5, *p<0.05 or **p<0.01 vs. CTL/EtOH. **C**. Representative images of co-labeling with TUNEL (green) and CHOP (red) in CC, CA1, and CB sections of PD7 pups from the cKO/EtOH group. Scale bar: 20um. **D**. Representative immunoblots of ER stress markers (GRP78, CHOP, XBP1s and ATF6) in the entire brains of PD7 pups from control (CTL/mock and CTL/TM) and cKO (cKO/TM) groups. n=3–5, *p<0.05 vs. CTL/mock. #p<0.05 or ##p<0.01 vs. CTL/TM. **E**. Representative staining of CHOP (brown) and Hematoxylin (blue) in CC, CA1, and CB sections of PD7 pups from control CTL/TM and cKO/TM groups. Scale bar: 20um. n=3–5, *p<0.05 or **p<0.01 vs. CTL/TM.

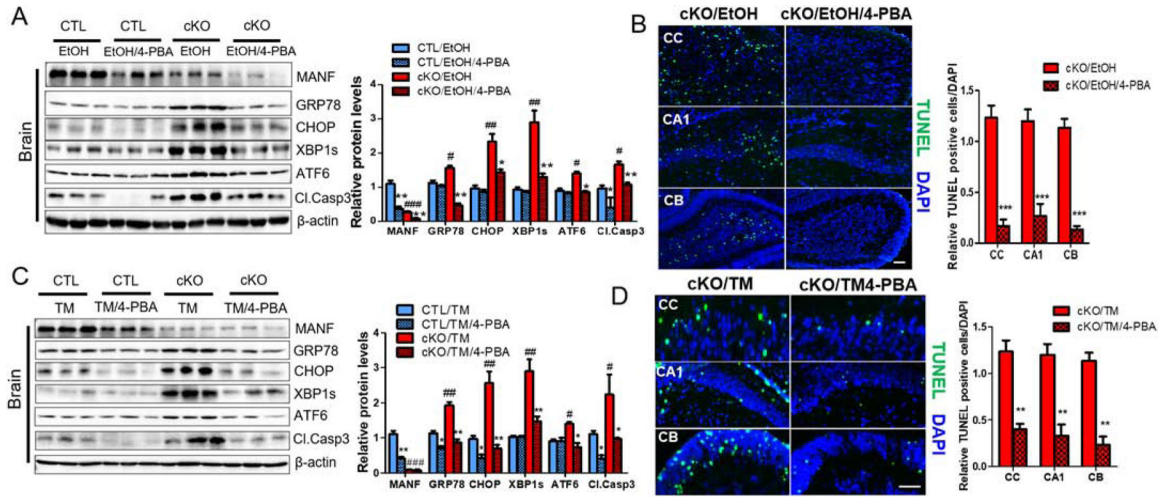

Figure 7. Blocking ER stress abrogates the deleterious effects of MANF deficiency on ethanol- and TM-induced neuronal apoptosis.

A. Representative immunoblots of ER stress markers and Cl. Casp 3 in the whole brains of PD7 pups from the control (CTL/EtOH and CTL/EtOH/4-PBA) and cKO (cKO/EtOH and cKO/EtOH/4-PBA) groups. n=3–5, *p<0.05 or **p<0.01 vs. corresponding treatment control (CTL/EtOH or cKO/EtOH) groups. #p<0.05 or ##p<0.01 vs. CTL/EtOH. **B**. Representative images of TUNEL (green) and DAPI (blue) labeling in CC, CA1, and CB sections of PD7 pups from cKO/EtOH and cKO/EtOH/4-PBA groups. Scale bar: 20 um. n=3–5, ***p<0.001 vs. cKO/EtOH. **C**. Representative immunoblots of ER stress markers and Cl.Casp3 in the entire brains of PD7 pups from control (CTL/TM and CTL/TM/4-PBA) and cKO (KO/TM and KO/TM/4-PBA) groups. n=3–5, *p<0.05 or **p<0.01 vs. corresponding treatment control (CTL/TM or cKO/TM) groups. #p<0.05 or ##p<0.01 vs. CTL/TM. **D**. Representative images of TUNEL (green) and DAPI (blue) labeling in CC, CA1, and CB sections of PD7 pups from cKO/TM and cKO/TM/4-PBA groups. Scale bar: 20 um. n=3–5, **p<0.01 vs. cKO/TM.

Table 1.

Differentially expressed genes related to protein processing in the ER from RNA-Seq.

Gene Symbols	Transcripts per million (TPM)						Fold change*
	CTL1	CTL2	CTL3	cKO1	cKO2	cKO3	
EDEM3	10.59	0	0	0	0.03	0	−353
PDIA3	178.25	194.95	198.1	236.47	229.3	245.79	1.25
GRP78	190.45	210.63	200.87	325.24	321.53	373.94	1.70
RRBP1	0	0	0	5.73	0	0	3549
UBE2J2	3.62	2.7	0.56	0	0	0	−2870
PDIA6	106.21	125.87	111.92	168.65	177.94	175.76	1.52
DDOST	74.59	78.86	81.03	100.56	109.77	114.31	1.38
PDIA4	64.16	67.02	72.67	88.98	85.02	91.26	1.30
HSP90B1	281.12	335.28	308.45	463.05	428.79	472.81	1.48
DNAJC3	27.04	32.01	28.88	45.9	34.96	42.65	1.40
SEC61A1	77.17	81.16	81.32	96.02	94.07	105.29	1.23
ERLEC1	6.58	11.19	10.87	14.79	14.02	16.97	1.60
SELENOS	32.21	39.69	36.44	54.88	50.98	45.98	1.40
HY0U1	0	0	0	10.12	8.6	12.97	17439
SEC24D	10.82	15.53	15.35	19.93	19.17	19.79	1.41
UGGT1	14.51	16.23	16.71	20.55	19.63	24.6	1.37
UBXN6	8.03	6.79	4.52	0	0	0	−3004
ATF4	105.87	134.57	107.86	157	149.97	156.83	1.33

*, − and + indicate down- and up-regulation, respectively (cKO vs CTL).